Analytical Solutions Of The Perfect Absorber For Terahertz Sensing

P. Tapsanit[1,2], M. Yamashita[2], and C. Otani[1,2]
[1]Department of Physics, Tohoku university, Aoba-ku, Sendai, 980-8578, Japan
[2]RIKEN Center for Advanced Photonics, Aramaki-Aoba, Aoba-ku, Sendai, 980-0845, Japan.

***Abstract*—We develop the analytical solutions (ANS) of the hybrid structure comprising the metallic grating (MG) with subwavelength width, the stacked-dielectric layers in front of the MG, and one dielectric layer behind the MG. The ANS are well consistent with the finite difference time domain simulation. We apply the ANS to optimize the flat-surface front-perfect absorber (FPA) with ultrahigh Q-factor up to 3×10^4 based on the coupling between the quasi-waveguide resonance (QWR) and the Fabry-Perot (FP) resonance. The proposed FPA can detect the small variations in refractive indices of thin samples and the presence of thin films with deep-subwavelength thicknesses.**

I. INTRODUCTION

THE discovery of the extraordinary optical transmission (EOT) in a thick metallic film perforated by the small hole arrays has generated the immense interests in its basic properties and novel applications [1]. The complete theories of the EOT effect for the hole arrays [2] and the slit arrays [2,3] show that the coupling between the electromagnetic modes inside the cavities with the diffraction waves are responsible for the EOT effect. However, this coupled-mode (CM) analysis applies only to the structured metallic film bound by two semi-infinite input and output media, e.g. vacuum and substrate, and therefore it cannot be employed to study the hybrid structure which bring dielectric layers to become parts of the device.

In this work, the ANS of the hybrid structure comprising the MG, stacked-dielectric layers (SDL) attached in front of the MG, and one dielectric layer attached behind the MG are given by connecting the CM analysis with the transfer matrix method. We check the validity of the ANS with the finite difference time domain simulation (FDTD). We then apply the ANS to optimize the ultrahigh Q-factor FPA with flat surface of Si layer in front of the MG and Zeonex polymer filling the slit's cavity. The ultrasensitive sensing using this FPA is demonstrated by monitoring the absorption at the resonance. The ANS not only yield the highly efficient tools in the optimization of the perfect absorbers but will also inspire many new hybrid structures.

II. RESULTS

The hybrid structure is schematically shown in Fig. 1(a). The transverse magnetic (TM) wave with the amplitude of the incident magnetic field H_0 is incident on the structure from the input region. The dielectric layer attached behind the MG will be later defined as the metal to make the FPA. The metal is modeled as the perfect electric conductor (PEC) which is valid for THz and lower frequency radiation. The slit's width is assumed to be very small comparing to the wavelength of the incident light so that only the fundamental waveguide mode

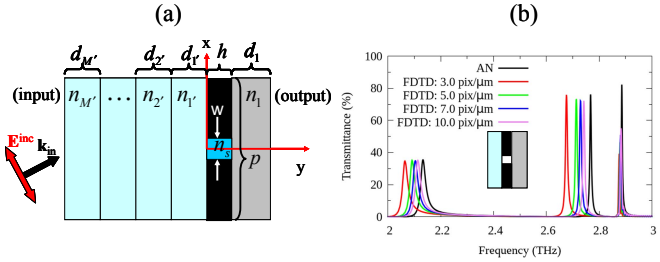

Fig. 1. (a) Schematic view of the unit cell of the hybrid structure comprising the MG, M number of SDL attached in front of the MG, and one dielectric layer behind the MG which later will be defined as a PEC layer making the FPA. (b) Comparison between the analytical and FDTD spectra of simple Si-MG-Teflon structure shown in the inset. The thicknesses of the Si and Teflon layers are defined as 10 μm. The dielectric constants of Si and Teflon with neglected losses are 11.7 and 2.088, respectively. The MG's parameters are defined as p=100 μm, w=h=1 μm, ε_s=1.

is excited inside the slit's cavity. This means that the magnetic field H_z is constant along the x-axis inside the slit's cavity, but it is propagating wave along the y-axis. The magnetic fields H_z in the remaining regions : reflected fields in the input region, internal fields in each of SDL of the input (denoted by the apostrophe) and the output sides, and the transmitted fields in the output region, are all expanded in terms of the Bloch's basis functions $\langle x|\beta_m\rangle = \exp(i\beta_m x)/\sqrt{p}$, where p is the slit period, $\beta_m = k_x + m2\pi/p$, $k_x = k_{\text{in}}\sin\theta$, and m is an integer. By applying the transfer matrix method which is actually equivalent to applying the continuities of H_z and E_x at the interfaces between two regions, all field coefficients of left- and right- travelling waves can be obtained and the dispersion relation describing the coupled-electromagnetic modes on two faces of the MG can be generally written as

$$\Omega = \left(G_{\infty s}^{(\text{in})} - \gamma\right) - G_V^2/\left(G_{\infty s}^{(\text{out})} - \gamma\right) = 0, \qquad (1)$$

where $\gamma = \cot(k_s h)$, $G_V = \csc(k_s h)$, and $G_{\infty s}^{(\text{in})}$ and $G_{\infty s}^{(\text{out})}$ are the scattering parameters of the CM in the input and output regions, respectively, defined as

$$G_{\infty s}^{(\text{in})} = i\frac{n_s\varepsilon_{1'}}{n_{1'}\varepsilon_s}\sum_{m=-\infty}^{\infty} W_m^{(\text{in})} Y_m^{(1')}(w/p)\,\text{sinc}^2(\beta_m w/2), \qquad (2)$$

$$G_{\infty s}^{(\text{out})} = i\frac{n_s\varepsilon_1}{n_1\varepsilon_s}\sum_{m=-\infty}^{\infty} W_m^{(\text{out})} Y_m^{(1)}(w/p)\,\text{sinc}^2(\beta_m w/2). \qquad (3)$$

If the functions $W_m^{(\text{in})} = W_m^{(\text{out})} = 1$, then the scattering parameters are reduced to the conventional forms in the CM theory (with $\varepsilon_{1'} = \varepsilon_{\text{in}}$ and $\varepsilon_1 = \varepsilon_{\text{out}}$) [2,3]. In our case, the $W_m^{(\text{in})}$ and $W_m^{(\text{out})}$ take into account the multiple reflections of the CM inside the dielectric layers and are defined as : $W_m^{(\text{in})} = \left(\bar{S}_{11}^{(m)} - \bar{S}_{12}^{(m)}\right)/\left(\bar{S}_{11}^{(m)} + \bar{S}_{12}^{(m)}\right)$, $W_m^{(\text{out})} = \left(1 + r_{1,\text{out}}^{(m)} e^{2i\phi_m^{(1)}}\right)/\left(1 - r_{1,\text{out}}^{(m)} e^{2i\phi_m^{(1)}}\right)$, where the matrix elements of the input scattering matrix,

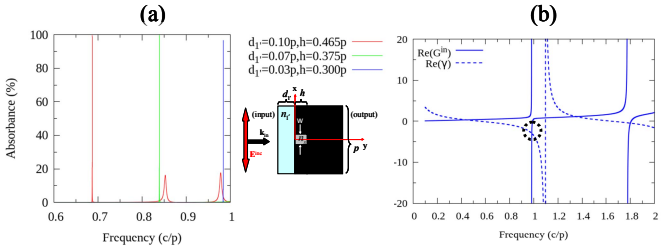

Fig. 2. (a) The analytical absorption spectra of the FPA schematically shown in the inset for three different Si layer's thicknesses and corresponding optimized slit's heights. (b) Real parts of $G_{\infty s}^{(\mathrm{in})}$ and γ for $d_{1'}$=0.03p, h=0.300p as a function of frequency.

$\bar{S}_{ij}^{(m)}$, is obtained by $\bar{\mathbf{S}}^{(m)} = \bar{\mathbf{T}}_{\mathrm{in},M'}^{(m)} \cdots \bar{\mathbf{T}}_{2',1'}^{(m)}$ with the input transfer matrix $\bar{\mathbf{T}}_{i',j'}^{(m)}$ defined as

$$\bar{\mathbf{T}}_{i',j'}^{(m)} = \begin{pmatrix} \exp\left(-i\phi_m^{(j')}\right) & r_{i',j'}^{(m)} \exp\left(i\phi_m^{(j')}\right) \\ r_{i',j'}^{(m)} \exp\left(-i\phi_m^{(j')}\right) & \exp\left(i\phi_m^{(j')}\right) \end{pmatrix}, \quad (5)$$

where $\phi_m^{(j')} = q_m^{(j')} d_{j'}$, $q_m^{(j')} = \sqrt{k_{j'}^2 - \beta_m^2}$, and $r_{i',j'}^{(m)}$ is the mth-order Fresnel-reflection coefficient. The mth-order Fresnel-reflection and transmission coefficients of TM waves from media a to b are defined as

$$r_{a,b}^{(m)} = \frac{\varepsilon_b q_m^{(a)} - \varepsilon_a q_m^{(b)}}{\varepsilon_b q_m^{(a)} + \varepsilon_a q_m^{(b)}}, \; t_{a,b}^{(m)} = \frac{2\varepsilon_b q_m^{(a)}}{\varepsilon_b q_m^{(a)} + \varepsilon_a q_m^{(b)}}. \quad (6)$$

The reflectance (R) and transmittance (T) are obtained by summing all propagating mth-order total reflection coefficient $B_m^{(\mathrm{in})}$ and total transmission coefficient $A_m^{(\mathrm{out})}$, respectively :

$$R = P\left\{\sum_m \left(\frac{q_m^{(\mathrm{in})}}{q_0^{(\mathrm{in})}}\right)\left|\frac{B_m^{(\mathrm{in})}}{H_0}\right|^2\right\}, \; T = \frac{\varepsilon_{\mathrm{in}}}{\varepsilon_{\mathrm{out}}} P\left\{\sum_m \left(\frac{q_m^{(\mathrm{out})}}{q_0^{(\mathrm{in})}}\right)\left|\frac{A_m^{(\mathrm{out})}}{H_0}\right|^2\right\}. \quad (7)$$

Here, we show only the analytical expression of the reflection coefficient which can be explicitly written as

$$\frac{B_m^{(\mathrm{in})}}{H_0} = e^{-i\phi_0^{(\mathrm{in})}}\left(\frac{\bar{S}_{22}^{(0)} + \bar{S}_{21}^{(0)}}{\bar{S}_{12}^{(0)} + \bar{S}_{11}^{(0)}}\right)\delta_{m0} + \frac{2I_0 e^{-i\phi_0^{(\mathrm{in})}}}{\Omega}\left(\frac{t_{\mathrm{in},M'}^{(0)} \cdots t_{2',1'}^{(0)}}{\bar{S}_{12}^{(0)} + \bar{S}_{11}^{(0)}}\right)\frac{1}{t_{\mathrm{in},M'}^{(m)} \cdots t_{2',1'}^{(m)}}, \quad (8)$$

$$\times\left(\frac{\det\left(\bar{\mathbf{S}}^{(m)}\right)}{\bar{S}_{12}^{(m)} + \bar{S}_{11}^{(m)}}\right)\left(\frac{n_s \varepsilon_{1'}}{n_{1'} \varepsilon_s}\right) i Y_m^{(1')} \sqrt{\frac{w}{p}} \operatorname{sinc}\left(\beta_m w/2\right)$$

where $I_0 = -\sqrt{w/p}\operatorname{sinc}\left(\beta_m w/2\right)$, and $\phi_0^{(\mathrm{in})} = q_0^{(\mathrm{in})} \sum_{j=1}^{M} d_{j'}$

In order to validate the ANS, we calculate the spectra of the simple Si-MG-Teflon hybrid structure shown in the inset of Fig. 1(b) by using FDTD simulation, and the transmission spectra from two methods are compared in Fig. 1(b). It can be seen that resonant peaks from the FDTD spectra approach those from analytical spectra by increasing the resolutions. We notice that the resonant frequency of the third peak from the lower energy side is almost the same for ANS and FDTD (ANS : 2.886 THz, FDTD(10) : 2.883 THz). This peak is the 1st-order QWR in Teflon layer which is induced by the m=1 quasi-Wood's anomaly at which the transmittance is exactly zero. The QWR scatters the zero-order reflected wave anti-parallel to the incident light (π-phase difference) and therefore the electromagnetic wave can transmit through the structure in order to conserve the energy. Similarly, the first and second peaks are the 1st-order and 3rd-order QWR in the Si layer, respectively, which are induced by the m=1 and m=2 quasi-Wood's anomaly, respectively. Therefore, the large dielectric constant of Si layer requires higher resolutions in order to accurately obtain the resonant frequency by FDTD.

Now, we define the dielectric layer 1 behind the MG as PEC ($\varepsilon_1 \to -\infty + i\infty$), fill the slit with lossy Zeonex poymer [5], and attach Si layer in front of the MG to make the FPA. The parameter $G_{\infty s}^{(\mathrm{out})}$ of the FPA becomes infinity, the dispersion function is reduced to $\Omega_{\mathrm{FPA}} = G_{\infty s}^{(\mathrm{in})} - \gamma$, and the transmittance is zero. Fig. 2(a) shows the nearly perfect absorption peaks of the FPA excited by normal incident TM wave for three Si layer's thicknesses $d_{1'}$ equal to 0.03p, 0.07p, and 0.10p, with corresponding optimized slit's heights equal to 0.300p, 0.375p, and 0.465p, respectively. In order to understand the origin of the sharp peaks, we plot the $\mathrm{Re}\left(G_{\infty s}^{(\mathrm{in})}\right)$ and $\mathrm{Re}(\gamma)$ for $d_{1'}$ =0.03p, h=0.300p in Fig. 2(b). The resonant frequency of this FPA occurs at the crossing point marked by the dotted circle close to the m=1 quasi-Wood's anomaly and the first-order FB. Therefore, the quasi-Wood's anomaly introduces the QWR which can be coupled to the FBR generating the perfect absorption and the ultrahigh Q-factor equal to 30,267 for this peak. The Q-factors of the green and red peaks in Fig. 2(a) are 5,992 and 3,505, respectively. The smaller Q-factor occurs because the difference between $\mathrm{Re}\left(G_{\infty s}^{(\mathrm{in})}\right)$ and $\mathrm{Re}(\gamma)$ around the resonant frequency becomes more slowly changes. By monitoring absorbance at the resonant frequency of the highest Q-factor FPA due to the presence of a thin sample with thickness 0.01p, we find that the absorbance decreases by 50% due to the variation in refractive index of the sample 0.69x10^{-3} RIU. Moreover, the absorbance decreases by 50% at the resonant frequency of the same FPA due to the presence of $n_{2'}$=1.6 film with thickness 2.13x10^{-5}p. This gives the opportunity of using THz light to sense the nanofilms.

III. Summary

The ANS of the FPA which are consistent with FDTD simulation are given. The FPA with ultrahigh Q-factor about 3x10^4 is achieved by coupling the QWR in Si layer with the FB in the Zeonex slit's cavity. The ultrahigh Q-factor FPA allows the ultrasensitive detection of the variations in refractive indices and thicknesses of thin films.

References

[1]. T. W. Ebbensen, H. J. Lezec, H. F. Ghaemi, T. Thio, and P. A. Wolff, "Extraordinary optical transmission through sub-wavelength hole arrays," Nature 391, pp. 667-669, (1998).

[2]. F. J. García-Vidal, L. Martín-Moreno, T. W. Ebbensen, and L. Kuipers, "Light passing through subwavelength apertures," Rev Mod. Phys. 82(1), 729-787, (2010).

[3]. A. I. Fernández-Domínguez, F. J. García-Vidal, and L. Martín-Moreno, "Resonant transmission of light through finite arrays of slits," Phys. Rev. B 76, 235430 (7pp), (2007).

[4] A. F. Oskooi, D. Roundy, M. Ibanescu, P. Bermel, J. D. Joannopoulos, and S. G. Johnson, Comput. Phys. Commun. **181**(3), 687-702, (2001).

[5] J. Anthony, R. Leonhardt, A. Argyros, and M. C. J. Large, "Characterization of a microstructured Zeonex terahertz fiber," J. Opt. Soc. Am. B **28**(5), 1013-1018, (2011).